1 *Article*

2 # Pentanuclear Hetero-bimetallic 3d-4f Complexes of

3 # the Ln$_2$Ni$_3$ type: Pr$_2$Ni$_3$ and Gd$_2$Ni$_3$

4 **Jana König,[1] Alexandra Kelling,[1] Uwe Schilde,[1] Peter Strauch,[1, †] and Andreas Taubert [1,*]**

5 [1] University of Potsdam, Institute of Chemistry, Karl-Liebknecht-Str. 24-25, D-14476 Potsdam, Germany

6 [*] Correspondence: University of Potsdam, Institute of Chemistry, Karl-Liebknecht-Str. 24-25, D-14476

7   Potsdam, Germany, ataubert@uni-potsdam.de; Tel.: +49-331-977-5773

8 [†] This work was performed as a part of the PhD thesis of Dr. Jana König under the supervision of Prof. Peter

9   Strauch. Peter Strauch passed away prematurely on July 15, 2017. We dedicate this article to the memory of

10   our long-time supervisor, collaborator, colleague, and friend.

11 **Abstract:** In aqueous solution planar bis(1,2-dithiooxalato)nickelates(II), $[Ni(dto)_2]^{2-}$ react with

12 lanthanide ions (Ln^{3+}) to form pentanuclear, hetero-bimetallic complexes of the general composition

13 $[\{Ln(H_2O)_n\}_2\{Ni(dto)_2\}_3] \cdot x\ H_2O$ (n = 4 or 5; x = 9 - 12). Two complexes of this series,

14 $[\{Pr(H_2O)_5\}_2\{Ni(dto)_2\}_3] \cdot 11\ H_2O$, Pr$_2Ni_3$ **1** and $[\{Gd(H_2O)_5\}_2\{Ni(dto)_2\}_3] \cdot 11\ H_2O$, Gd$_2Ni_3$ **2** were

15 synthesized and characterized by single crystal X-ray structure analysis, X-ray powder diffraction,

16 and IR spectroscopy. All Ln$_2$Ni$_3$ complexes crystallize as monoclinic crystals in the space group

17 $P2_1/c$.

18 **Keywords:** lanthanides, 1,2-dithiooxalate, crystal structure, nickel(II)

19

20 ## 1. Introduction

21   During the last decades molecular hetero-bimetallic 3d - 4f complexes with transition metals and

22 trivalent lanthanide ions have attracted increasing interest for their magnetic properties [1-16].

23 Besides magnetism, 3d-4f complexes are promising precursors for e.g. catalysts [17, 18] and

24 luminescent materials [18-23]. Since lanthanide ions have a large angular momentum and the f - f

25 transition is less influenced by the ligand field compared to the spin-orbit coupling, f-elements show

26 a magnetic behavior that is different from the transition metals [1]. Although the scientific and

27 technological interest of d-f hybrids is evident, the design and construction of extended hetero-

28 nuclear d-f complexes with a well-defined, discrete multinuclear organization is still a synthetic

29 challenge and new approaches towards these interesting materials are highly sought after. A few d-

30 f hybrids were synthesized in organic media, mostly because the ligands were not water-soluble [24,

31 25]. Most of the syntheses were done under hydrothermal conditions, usually using longer reaction

32 times of a few days [18, 20, 22, 26-29].

33   A ligand of interest for the synthesis of d-f hybrids is 1,2-dithiooxalate [30], a small bridging

34 ligand with *S*, *S* and *O*, *O* donor sites which specifically enable the combination of transition metals

35 with lanthanide ions at moderate conditions (reaction times of 15 minutes and temperatures of about

36 50 °C). Indeed, a series of pentanuclear, hetero-bimetallic 3d - 4f complexes with 1,2-dithiooxalate

37 (dto) as the bridging ligand with the general composition $[\{Ln(H_2O)_n\}_2\{Ni(dto)_2\}_3] \cdot x\ H_2O$. (n = 4 or 5;

38 x = 9 - 12) was first described by Trombe et al. [31, 32]. These authors reported that the decreasing

39 ionic radii of the lanthanide ions favor the formation of different types of crystal structures. With

40 larger lanthanide ions (La - Dy), monoclinic crystals form while with smaller ions (Er, Yb) triclinic
41 crystals are observed. The solid state conductivities of these compounds is on the order of 10^8 to $2 \cdot$
42 $10^9 \ \Omega^{-1} \cdot cm^{-1}$ [31].

43   More recently, Strauch and coworkers have provided further data on these compounds [33-36].
44 The nickel-holmium analogue has been considered as the borderline case between the monoclinic
45 and the triclinic forms until recently. A recent study [37], however, has shown that this particular
46 compound also crystallizes in the monoclinic space group $P2_1/c$ and cannot longer be regarded as a
47 borderline case. Instead, this case confirms that the larger lanthanide ions lead to monoclinic rather
48 than triclinic crystals. The current study further completes the series and demonstrates that
49 $[\{Pr(H_2O)_5\}_2\{Ni(dto)_2\}_3] \cdot 11 \ H_2O$, Pr_2Ni_3 and $[\{Gd(H_2O)_5\}_2\{Ni(dto)_2\}_3] \cdot 11 \ H_2O$, Gd_2Ni_3 also crystallize
50 in the monoclinic space group $P2_1/c$. These data further confirm the hypothesis by Trombe et *al.* [31,
51 32] and the current study further broadens the pool of d-f hybrids based on the 1,2-dithiooxalate
52 ligand.

2. Results

54   As stated in the introduction, pentanuclear hetero-bimetallic complexes with larger lanthanide
55 ions (Ln = La^{3+}-Ho^{3+}) are isostructural and crystallize in the monoclinic space group $P2_1/c$ [33-36]. In
56 contrast, pentanuclear complexes with smaller lanthanide ions (Ln = Er^{3+} - Lu^{3+}) crystallize in the
57 triclinic space group $P\bar{1}$ [33, 36]. In addition to X-ray diffraction, both subgroups can be distinguished
58 by X-ray powder diffraction (XRD) and IR spectroscopy [33-36]. We will thus first present the
59 crystallographic information and the IR data and finally also show the magnetic susceptibility data.

60 *2.1. Single crystal X-ray structures*

61   Single crystals of the complexes Pr_2Ni_3 **1** and Gd_2Ni_3 **2** were obtained from aqueous solutions
62 covered with hexane leading to the precipitation of dark purple crystals with a prismatic habit. Table
63 1 summarizes the crystallographic data and refinement parameters for the complexes.

70   **Table 1.** Crystallographic data and refinement parameters for the complexes **1** and **2**.

Compound	1	2
CCDC No.		

Empirical formula	$C_6H_{21}Ni_{1.5}O_{16.5}PrS_6$	$C_6H_{21}GdNi_{1.5}O_{16.5}S_6$
M / g·mol^{-1}	778.56	794.90
Crystal system	monoclinic	monoclinic
Space group	$P2_1/c$	$P2_1/c$
a / Å	10.1212(4)	10.3170(6)
b / Å	11.4036(5)	11.3872(7)
c / Å	20.6044(9)	20.5911(14)
α / °	90	90
β / °	98.298(3)	98.762(5)
γ / °	90	90
V / Å^3	2353.22(17)	2390.8(3)
Z	4	4
F(000)	1544	1564
Density / g·cm^{-3}	2.198	2.208
μ / mm^{-1}	3.836	4.511
Crystal size	0.04 x 0.13 x 0.24	0.10 x 0.17 x 0.21
Θ / °	2.00 - 25.00	2.00 - 25.00
R_{int}	0.0921	0.0641
Refl. measured	23178	30225
Refl. independent	4141	4201
Parameters	263	263
R_1 / wR_2 [$I > 2\sigma(I)$]	0.0460 / 0.1190	0.0258 / 0.0605
R_1 / wR_2 (all data)	0.0593 / 0.1259	0.0310 / 0.0622
Goodness of fit on	1.053	1.015
max. diff. peak / hole /e·Å^{-3}	0.758 / -1.437	0.806/ -0.707

71   Figure 1 shows the molecular structure of the pentanuclear hetero-bimetallic Gd$_2$Ni$_3$ complex **2**
72   with the characteristic z-shape (figure 2) of this type of molecules [33-37]. Two lanthanide centers are
73   bridged by a nearly planar bis(1,2-dithiooxalato)nickelate(II) unit through two *O, O* donor sets. Two
74   peripheric bis(1,2-dithiooxalato)nickelate(II) moieties are coordinated only bidentate in a non-
75   bridging mode. Each nickel(II) ion has a square-planar NiS_4 coordination sphere due to the
76   coordination of two sulfur donor atoms of two 1,2-dithiooxalato ligands. The lanthanide ions have a
77   coordination number of 9, which is achieved by four oxygen atoms of two 1,2-dithiooxalato ligands.
78   The coordination sphere is completed by five water ligands at each lanthanide ion. The nine donor
79   atoms in the coordination sphere of the lanthanide ion occupy the corners of a tricapped trigonal
80   prism. The molecule is centrosymmetric with a crystallographic inversion center on the Ni1-atom.
81   The complex is close to planar and only shows a slight out-of-plane twist due to the non-symmetric
82   coordination geometry at the lanthanide ions (Figure 2).
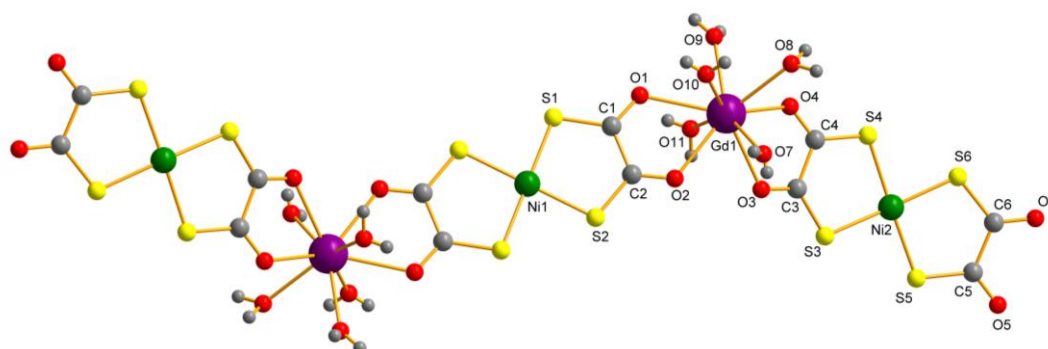
Figure 1. Molecular structure of the Gd$_2$Ni$_3$ complex **2**, view along the crystallographic *a* axis. Only the atoms of the asymmetric unit are labelled. Non-coordinated water molecules are omitted for clarity.

The crystal packing is presented in Figure 2. Channels and cavities, which are filled with non-coordinated water molecules can be observed. In contrast to the water molecules coordinated to the lanthanide ions, non-coordinated water molecules are strongly disordered. Therefore the SQUEEZE procedure of the program PLATON was used to subtract the contribution of the disordered water molecules from the structure factor calculations, for details see the Methods section below. PLATON/SQUEEZE calculated the solvent-accessible void volume and the number of electrons, corresponding to about 5.5 molecules of water per asymmetric unit. For the isostructural Pr$_2$Ni$_3$ complex **1** the same result was found.

The packing is stabilized by a large number of hydrogen bonds. The slightly varying number of non-coordinated water molecules could be estimated by thermogravimetric analysis. From previous experiments, it was determined with approximately 9 - 12 water molecules per formula unit in the Ce$_2$Ni$_3$-complex [34]. This weakly bound water is already partly released in dry laboratory air; this thus generates difficulties to determine their exact number. This effect is also responsible for the relatively high remaining electron density for this type of complexes.
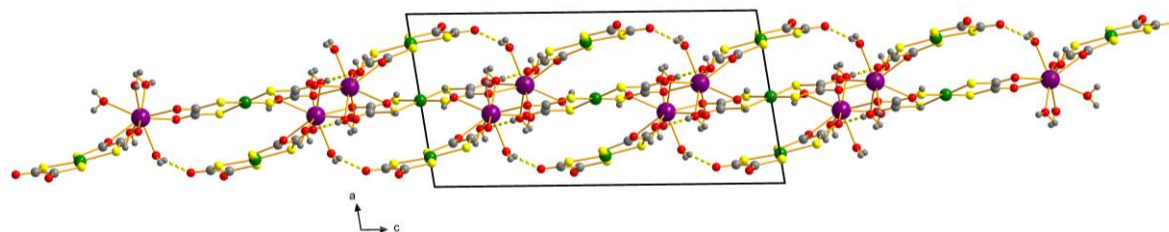
Figure 2. Packing diagram of the Gd$_2$Ni$_3$ complex **2**, without non-coordinated disordered water molecules. Hydrogen bonds as yellow dashed lines. View along the crystallographic *b* axis.

105　　　　　　　　　　　　**Table 2.** Selected bond lengths and angles of Pr$_2$Ni$_3$ **1** and Gd$_2$Ni$_3$ **2**.

	1	2
Coordination sphere of Ln^{3+} / Å		
Ln-O1	2.513(5)	2.533(3)
Ln-O2	2.590(5)	2.456(3)
Ln-O3	2.596(5)	2.542(3)
Ln-O4	2.524(5)	2.464(3)
Coordination sphere of Ni^{2+} / Å		
Ni1-S1	2.1787(16)	2.1724(9)
Ni1-S2	2.1717(16)	2.1848(10)
Ni2-S3	2.1997(18)	2.2016(11)
Ni2-S4	2.178(2)	2.1769(12)
Ni2-S5	2.182(2)	2.1807(11)
Ni2-S6	2.1788(18)	2.1776(11)
Terminal ligand / Å		
C5-C6	1.530(10)	1.536(6)
C5-O5	1.231(9)	1.228(5)
C6-O6	1.236(8)	1.226(5)
C5-S5	1.711(7)	1.712(4)
C6-S6	1.714(7)	1.704(4)
Bridging ligands / Å		
C1-C2	1.510(10)	1.521(5)
C3-C4	1.520(9)	1.525(5)
C1-O1	1.238(8)	1.251(4)
C2-O2	1.247(8)	1.247(4)
C3-O3	1.262(8)	1.257(4)
C4-O4	1.255(8)	1.233(5)
C1-S1	1.693(6)	1.695(4)
C2-S2	1.692(7)	1.686(4)
C3-S3	1.687(7)	1.693(4)
C4-S4	1.689(6)	1.687(4)
Intramolecular distances / Å		
Ln-Ni1	6.2689(5)	6.2216(6)
Ln-Ni2	6.2657(10)	6.2140(6)
Ln-Ln	12.5378(8)	12.4431(10)
Ni1-Ni2	11.4022(9)	11.3836(8)
Intermolecular distances / Å		
Ln⋯Ln	6.2919(6)	6.2640(5)
Bite angles / °		
O1-Ln-O2	61.98(16)	63.47(9)
O3-Ln-O4	61.68(14)	62.78(9)
S1-Ni1-S2	92.87(6)	92.57(4)
S3-Ni2-S4	91.93(7)	91.92(4)
S5-Ni2-S6	91.91(7)	91.76(4)

106

107 *2.3. Powder diffraction*

108   Complementary X-ray powder diffraction (XRD) data (not shown) confirm the above
109 crystallographic assignments. All patterns exhibit sharp reflections and enable a simplified
110 identification of the members of the two Ln_2Ni_3 crystallographical subgroups. XRD data of both the
111 Gd_2Ni_3 and the Pr_2Ni_3 variants studied here show patterns that can be assigned to a monoclinic space
112 group.

113 *2.2. IR spectroscopy*

114   Table 3 shows selected IR absorption bands of Pr_2Ni_3 **1**, Gd_2Ni_3 **2** as well as the corresponding
115 signals from Ho_2Ni_3 and Er_2Ni_3 [33, 36, 37]. Broad bands at approx. 3200 cm^{-1} can be assigned to OH
116 vibrations of water molecules in the channels and water molecules coordinated to the lanthanide
117 ions. Furthermore a broad vibration stemming from the carboxylate groups of the organic ligand at
118 approx. 1495 cm^{-1} is visible. The breadth is due to the overlap of different types of coordinated and
119 non-coordinated carboxylate groups: (1) vibrations of non-coordinated terminal carboxylate groups
120 of 1,2-dithiooxalato ligands, which are observed at approximately 1600 cm^{-1} (similar to the red form
121 of the mononuclear $K_2[Ni(dto)_2]$ complex [38]), (2) vibrations of carboxylate groups coordinated to
122 the lanthanide ions, (3) formation of intermolecular hydrogen bonds towards some of the carboxylate
123 groups and non-coordinated water molecules. Typical deformation vibrations (δ_{Ln-O}) are observed in
124 the range of 630-660 cm^{-1} typical deformation vibrations occur [39-41].

125   **Table 3.** Vibration bands in selected Ln_2Ni_3 complexes.

compound	ν_{O-H} (broad)	ν_{C-O} (broad)	ν_{C-C}, ν_{C-S}	ν_{C-C-S}	ν_{C-S}, $\delta_{O=C-S}$	δ_{Ln-O} [39-41]	ν_{Ni-S}
Pr_2Ni_3	3306	1492	1136	1093	989	629	440
Gd_2Ni_3	3327	1496	1140	1092	990	680	456
Ho_2Ni_3 [37]	3166	1490	1138	1108	990	671	458
Er_2Ni_3 [42]	3361	1501	1146	1094	1001	740	468

126 *2.4. Room temperature magnetic susceptibility*

127   The 4f electrons orbitals are well shielded by the occupied 5s and 5d orbitals. As a result the
128 lanthanide ions, coordinated in complexes and compounds, behave magnetically very close to free
129 ions [43]. Due to the small cooperative effect of the two lanthanide ions in the complexes slightly
130 higher magnetic moments for the complexes **1**, **2** can be estimated (see Table 4). The overall magnetic
131 moments can be calculated by a simple single ion approximation (equation 1) [44]:

$$\mu_{eff.}^2 = \mu_{eff.}(Ln1)^2 + \mu_{eff.}(Ln2)^2 \qquad\qquad\qquad\qquad (1)$$

132   In this case only the lanthanide ions contribute to the magnetic moments because the nickel(II)
133 ions of the complexes have a square planar coordination geometry with no significant axial contacts;

134   as a result, they are diamagnetic. Indeed, the magnetic moments obtained at room temperature for
135   the complex series with nickel(II) is in principle known [33, 35]. The current results are in good
136   agreement with the calculated values. Deviations are due to paramagnetic impurities of the used
137   lanthanide educts.

138   **Table 4.** Experimental and calculated magnetic moments of complexes **1** and **2**, as well as
139   values for the free Ln^{3+} ions at room temperature.

	μ_{eff}. [B.M.]		
	free ion (Ln^{3+}) [43]	calculated (equation 1)	measured
Pr_2Ni_3 **1**	3.58	5.06	4.61
Gd_2Ni_3 **2**	7.94	11.23	11.19

3. Discussion

141   Already in the 1980s, *Trombe et al.* investigated compounds combining the 3d transition metal
142   nickel with 4f lanthanide ions. These studies focused on the organic ligand K_2dto with its bridging
143   and chelating properties [31, 32]. Because of the symmetrical arrangement of two sulfur and two
144   oxygen atoms the coordination of thiophilic nickel ions and oxophilic lanthanide ions is dictated by
145   the ligand. The first crystal structure of an Ln_2Ni_3 complex, [{Eu(H$_2$O)$_5$)$_2$}{Ni(dto)$_2$]}$_3$] · x H$_2$O (10 ≤ x ≤
146   12), was reported in 1982 showing that this compound crystallizes in the monoclinic space group
147    $P2_1/c$ [31]. On the basis of this crystal structure, *Trombe et al.* already in 1982 postulated the existence
148   of two different types of crystal structures depending on the radii of the lanthanide ions: La^{3+}-Dy^{3+}-
149   based compounds should likely crystallize in the monoclinic space group $P2_1/c$. In contrast, Er^{3+}-Yb^{3+}-
150   based compounds should crystallize in the triclinic space group $P\bar{1}$. Indeed, two years later the crystal
151   structure of Yb_2Ni_3 further supported this postulate [98]. The same authors also postulated that the
152   transition between the two groups (monoclinic vs. triclinic) should occur at Dy_2Ni_3 [31, 32]. This early
153   assumption, however, was disproven by *König et al.* who showed that the Ho_2Ni_3 complex still
154   crystallizes in the monoclinic space group $P2_1/c$ [37].

155   All neutral pentanuclear heterobimetallic complexes, independent of the crystal system, are
156   centrosymmetric with a crystallographic inversation center on the Ni1-atom with a characteristic z-
157   shape. The shape is the result of the non-symmetric coordination geometry of the lanthanide ions
158   with their high coordination numbers. For all complexes, which crystallize in the monoclinic space
159   group the coordination number of the lanthanide ion is nine, for the triclinic space group the
160   coordination number is eight. Thereby, two thiophilic nickel(II) ions were coordinated by two 1,2-
161   dithiooxalate ligands through two *S, S* donor sets, so nearly planar [Ni(dto)$_2$]$^{2-}$ building blocks were
162   generated. Two of these building blocks with their non-coordinated terminal *O,O* donor sets are able
163   to coordinate at one lanthanide ion. In fact, each lanthanide ion is then coordinated by one terminal
164   [Ni(dto)$_2$]$^{2-}$ building block and one bridging [Ni(dto)$_2$]$^{2-}$ building block, which connect both
165   lanthanide ions to the resulting neutral pentanuclear Ln_2Ni_3 complex (figure 1). The saturation of the
166   free coordination units is achieved by water ligands.

167 All complexes crystallizing in the monoclinic crystal system behave like Pr_2Ni_3 **1** and Gd_2Ni_3 **2**.
168 Therefore, only the complex Gd_2Ni_3 **2** is discussed in detail. Gd^{3+} shows a coordination number of
169 nine, so the saturation of the coordination sphere is realized by the coordination of five water
170 molecules. The nine *O* donor atoms in the direct environment of the lanthanide ion exhibit a distorted
171 tricapped trigonal prism (figure 1). The nickel ions always show a nearly square planar coordination
172 behavior. The environment and the geometry of the coordinated nickel ions changed only slightly
173 after coordination to Gd(III), whereby the terminal and the bridging $[Ni(dto)_2]^{2-}$ building blocks are
174 only distinguished in terms of the bite angles S-Ni-S.

175 All bond lengths Ni-S are in the range of 2.17-2.21 Å. Compared with the homoleptic complexes
176 $K_2[Ni(dto)_2]$ [45] and $(Ph_4P)_2[Ni(dto)_2]$, $(Ph_4As)_2[Ni(dto)_2]$ [46] the bond lengths are somewhat longer,
177 which is explainable with the additional coordination of the lanthanide ion at the same building block
178 $[Ni(dto)_2]^{2-}$ and therefore with the changing of electron density distribution inside the ligands. The
179 bite angles S1-Ni1-S2 in the range of 92.0-93.0 ° are somewhat bigger than the terminal bite angles S3-
180 Ni2-S4 and S5-Ni2-S6 (91.7-92.0 °). The building block $[Ni(dto)_2]^{2-}$, with Ni1 in its center, is chelated
181 by two lanthanide ions on each side. The *S* donor atoms as well as the *O* donor atoms of the 1,2-
182 dithiooxalate ion coordinates any metal center, whereby the situation is the same as in the
183 mononuclear complex $K_2[Ni(dto)_2]$ [45] with similar bite angles S-Ni-S, where also *S* and *O* donor
184 atoms are coordinated at either Ni or K. The terminal $[Ni(dto)_2]^{2-}$ building blocks do not have a
185 coordination partner at the *O, O* donor set of the 1,2-dithiooxalate ligands. Therefore they behave like
186 $(Ph_4P)_2[Ni(dto)_2]$ and $(Ph_4As)_2[Ni(dto)_2]$ [46], because also the homoleptic complexes with organic
187 counter ions are not coordinated at the *O, O* donor sets of the 1,2-dithiooxalate ligands. The resulting
188 Gd-O bond lengths after chelation are in good agreement with calculated bond lengths as a sum of
189 the effective radius of gadolinium with a coordination number of nine and the ionic radius of O^{2-} with
190 a coordination number of two as a guide value [47, 48].
191 The terminal and bridging ligands exhibit C-C bond lengths typical of sp^2-hybridized carbon
192 atoms, analogous to the non-coordinated ligand K_2dto [49] and the ligand in the homoleptic
193 complexes [45, 46]. The S-C bond lengths are between single bonds and double bonds. This supports
194 the interpretation that the electrons are delocalized in the peripheral O-C-S units of the ligands after
195 coordination to the nickel ions. The C-O bond lengths differ from each other depending on the
196 coordination situation inside the complex. The bridging ligands show extended C-O double bonds
197 due to the coordination to the gadolinium ion. The terminal C-O bonds are nearly perfect double
198 bonds because of the non-coordination situation on the *O,O* donor sets.

199 Complexes crystallizing in the triclinic space group $P\bar{1}$ show the same coordination geometry
200 around the nickel(II) as in the monoclinic crystals. The coordination number of the lanthanide ions,
201 however, decreases from 9 to 8. The saturation of the coordination sphere of the lanthanide is
202 achieved by four oxygen atoms from the 1,2-dithiooxalate ligand and by the coordination of four
203 (instead of five) oxygen atoms from coordinated water molecules. The coordination geometry of the
204 two bridging 1,2-dithiooxalato ligands remains unchanged and the planarity is essentially driven by
205 the now symmetric coordination geometry at the lanthanide ions (compared figure 1B). With
206 decreasing ionic radii of the lanthanide ions from La^{3+} up to Lu^{3+} decreasing of coordinative bonds
207 between oxygen of the ligand and lanthanide ions and increasing of bite angles between chelating

208   ligands and lanthanide ions will be observed. This is explainable by a better overlap of orbitals which
209   take part in bindings. Bite angles increase by approximately 0.3 degrees within the range of the
210   monoclinic subgroup. The change from a coordination number of 9 (monoclinic) to 8 (triclinic)
211   significantly reduces the steric hindrance; this directly affects the bite angle, which increases by about
212   3 degree from Ho_2Ni_3 (last monoclinic complex) to Er_2Ni_3 (first triclinic complex). Within the triclinic
213   crystals the bite angles increase by approximately 0.3 degrees again.

214   IR spectroscopy is a very efficient complementary method able to distinguish between the two
215   crystal systems. Numerous vibration bands (ν_{C-C}/ ν_{C-S}, ν_{C-S}/ $\delta_{O=C-S}$, ν_{Ni-S}) blue-shift by approximately 10
216   cm^{-1} upon transitioning from the monoclinic (cn (Ln^{3+}) = 9) to the triclinic (cn (Ln^{3+}) = 8) crystal system
217   (table 3). This suggests that the better overlap of orbitals and the decreasing steric hindrance leads to
218   a stronger binding in the triclinic compounds.

219   The magnetic susceptibilities (Table 4) of the current compounds at room temperature are
220   comparable to similar examples in the literature [33, 35].

4. Materials and Methods

221

222   **Materials**. Oxalylchloride (Sigma-Aldrich, ≥ 98 %), phenol (Riedel-de Häen, ≥ 99,5 %), pyridine
223   (Acros organics, ≥ 99 %), potassium (Merck, ≥ 98 %), ethanol (Roth, ≥ 99,8 %), iron sulfide (Merck),
224   hydrochloric acid (VWR, 35 %), $NiCl_2 \cdot 6 H_2O$ (ChemPur, 98 %), $PrCl_3 \cdot x H_2O$ (ChemPur, 99,9 %), and
225   $GdCl_3 \cdot x H_2O$ (ChemPur, 99,9 %) were used as received. Chloroform (J. T. Baker, ≥ 99 %) was dried
226   over $CaCl_2$ prior to synthesis.

227   **Methods**. All infrared spectra were recorded on a Perkin Elmer 16PC FT-IR-spectrometer
228   between 400 and 4000 cm^{-1} using KBR pellets. Elemental analysis (C, H, S) was done on a Vario EL III
229   CHNS (elementar Analysensysteme GmbH, Hanau, Germany). Magnetic susceptibility
230   measurements were done on a magnetic susceptibly balance MBS-Auto (Sherwood Scientific Ltd.) at
231   room temperature. XRD measurements were done with a Bruker AXS (Siemens) D5005
232   diffractometer using CuK_α radiation (λ = 1.540598 Å, 2θ range: 3 – 70°, step size: 0.02°).

233   X-ray structures were determined using a STOE Image Plate Diffraction System IPDS-2 at 210 K
234   with graphite-monochromatized MoK_α radiation. The reflection data were corrected for absorption
235   as well as for Lorentz and olarization effects using the program X-Area [50]. The structures were
236   solved by direct methods using SHELXS-2013/2 [51] and refined by full-matrix least squares on F^2
237   using the program SHELXL-2014/7 [52]. Molecular graphics were prepared with DIAMOND [53].
238   The non-hydrogen atoms were refined anisotropically. The positions of the hydrogen atoms of the
239   coordinated water molecules were calculated with the program OLEX2 [54]. In **1**, only the hydrogen
240   atoms on O7 were calculated, the others were found from difference fourier map. The crystal water
241   molecules show a high degree of disordering and could not be resolved satisfactorily.
242   PLATON/SQUEEZE [55] calculated a solvent-accessible void volume in the unit cell of 649 Å^3 (27.1
243   % of the total cell volume), corresponding to 222 electrons (residual electron density after the last
244   refinement cycle) per cell. The number agrees with about 5.5 molecules of water (5.5x10x4=220) per
245   asymmetric unit. For the Pr_2Ni_3 complex **1** a solvent-accessible void volume of 553 Å^3 (23.5 % of the

246 total cell volume), corresponding to 219 electrons cell, agreeing about 5.5 molecules of water
247 (5.5x10x4=220) per asymmetric unit were found, too. The hydrogen atoms of the high-disordered
248 water lattice molecules could been neither located from the difference Fourier map nor calculated in
249 the expected positions yielding satisfactory refinement results. The crystallographic data of **1** and **2**
250 were deposited and can be obtained free of charge from the Cambridge Crystallographic Centre via
251 www.ccdc.cam.ac.uk/data_request/cif.

252 **Synthesis**. Potassium 1,2-dithiooxalate, K_2dto, was synthesized by sulfhydrolysis of diphenyl
253 oxalate according to Matz and Mattes [56] modified by Wenzel et al. [57]. The complexes Pr_2Ni_3 and
254 Gd_2Ni_3 were prepared according to the general procedure described by Trombe et al. [32].

255 A solution of K_2dto (1 mmol, 200.2 mg) in 5 mL of distilled H_2O was added to a stirred solution
256 of $NiCl_2 \cdot 6\ H_2O$ (0.5 mmol, 119.7 mg) in 4 mL of distilled H_2O. The resulting dark-purple solution
257 was heated to 50 °C. A warm solution (50 °C) of $LnCl_3 \cdot x\ H_2O$ (0.33 mmol) ($Ln^{3+} = Pr^{3+}$, Gd^{3+}) in 4 mL
258 distilled water was added drop-wise to the stirred $[Ni(dto)_2]^{2-}$-solution. The resulting reaction
259 mixture was continuously stirred at 50 °C for additional 15 min, then slowly cooled to room
260 temperature. The dark-purple crystalline precipitate was filtered, washed with a small amount of
261 distilled water, and dried at 80 °C.

262 **K_2dto:** $C_2O_2S_2K_2$ (M = 198.35 g · mol^{-1}). Elemental analysis (EA) measured (calculated): C 12.11
263 (12.13); S 32.21 (32.35) %. IR (KBr): 1530, 1514 (ν_{C-O}); 1113 (ν_{C-C}, ν_{C-S}); 881 (ν_{C-S}); 697, 677 ($\gamma_{C-C-O-S}$); 579
264 (ν_{C-S}); 516 (δ_{O-C-S}) cm^{-1}.

265 **Pr_2Ni_3:** $C_{12}H_{40}O_{32}S_{12}Pr_2Ni_3$ (M = 1539.10 g · mol^{-1}). Elemental analysis (EA) measured (calculated):
266 C 9.18 (9.36); H 2.49 (2.62); S 25.05 (25.00) %. IR (KBr): 3306 (ν_{OH}), 1492 (ν_{C-O}), 1136, 1093 (ν_{C-C-S}), 989
267 (ν_{C-S}), 629 (δ_{Ln-O}), 440 (ν-S, δ_{ring}) cm^{-1}. μ_{eff} meas. (calc.): 4.61 (5.06) B.M.

268 **Gd_2Ni_3:** $C_{12}H_{44}O_{34}S_{12}Gd_2Ni_3$ (M = 1607.84 g · mol^{-1}). Elemental analysis (EA) measured
269 (calculated): C 8.98 (8.96); H 2.43 (2.67); S 21.41 (23.93) %. IR (KBr): 3327 (ν_{OH}), 1496 (ν_{C-O}), 1140, 1092
270 (ν_{C-C-S}), 990 (ν_{C-S}), 680 (δ_{Ln-O}), 456 (ν_{Ni-S}, δ_{ring}) cm^{-1}. μ_{eff} meas. (calc.): 11.19 (11.23) B.M.

271 **Supplementary Materials.**

274 **Author Contributions**: J.K. synthesized and characterized all compounds. A.K. and U.S. determined the
275 single crystal structures. J.K., P.S., U.S., and A.T. analyzed the data. P.S. supervised the work and J.K., P.S., and
276 A.T. wrote the manuscript. All authors except P.S. read, corrected, and approved the final manuscript before
277 submission.

278 **Conflicts of Interest:** The authors declare no conflict of interest.

279 # References

280 [1] C. Benelli, D. Gatteschi, *Chem. Rev.* **2002**, *102*, 2369-2387.

281   [2]   A. Caneschi, L. Sorace, U. Casellato, P. Tomasin, P. A. Vigato, *Eur. J. Inorg. Chem.*
282   **2004**, 3887-3900.

283   [3]   J.-P. Costes, F. Dahan, A. Dupuis, J.-P. Laurent, *Inorg. Chem.* **1996**, *35*, 2400-2402.

284   [4]   J.-P. Costes, F. Dahan, A. Dupuis, J.-P. Laurent, *Inorg. Chem.* **1997**, *36*, 4284-4286.

285   [5]   S. Decurtins, M. Gross, H. W. Schmalle, S. Ferlay, *Inorg. Chem.* **1998**, *37*, 2443-
286   2449.

287   [6]   T. Kido, Y. Ikuta, Y. Sunatsuki, Y. Ogawa, N. Matsumoto, *Inorg. Chem.* **2003**, *42*,
288   398-408.

289   [7]   R. Koner, G.-H. Lee, Y. Wang, H.-H. Wei, S. Mohanta, *Eur. J. Inorg. Chem.* **2005**,
290   1500-1505.

291   [8]   Y.-T. Li, C.-W. Yan, H.-D. Wang, *Polish J. Chem.* **2000**, *74*, 1655-1663.

292   [9]   A. Merca, A. Müller, J. v. Slageren, M. Läge, B. Krebs, *J. Clust. Sci.* **2007**, *18*, 711-
293   719.

294   [10]   I. Ramade, O. Kahn, Y. Jeannin, F. Robert, *Inorg. Chem.* **1997**, *36*, 930-936.

295   [11]   T. Sanada, T. Suzuki, S. Kaizaki, *J. Chem. Soc.* **1998**, 959-965.

296   [12]   T. Sanada, T. Suzuki, T. Yoshida, S. Kaizaki, *Inorg. Chem.* **1998**, *37*, 4712-4717.

297   [13]   J. L. Sanz, R. Ruiz, A. Gleizes, F. Lloret, J. Faus, M. Julve, J. J. Borra´s-Almenar, Y.
298   Journaux, *Inorg. Chem.* **1996**, *35*, 7384-7393.

299   [14]   W. Shi, X.-Y. Chen, B. Zhao, A. Yu, H.-B. Song, P. Cheng, H.-G. Wang, D.-Z. Liao,
300   S.-P. Yan, *Inorg. Chem.* **2006**, *45*, 3949-3957.

301   [15]   S. Tanase, J. Reedijk, *Chem. Rev.* **2006**, *250*, 01-2510.

302   [16]   S. Osa, T. Kido, N. Matsumoto, N. Re, A. Pochaba, J. Mrozinski, *J. Am. Chem. Soc.*
303   **2004**, *126*, 420-421.

304   [17]   F. Evangelisti, R. More, F. Hodel, S. Luber, G. R. Patzke, *J. Am. Chem. Soc.* **2015**,
305   *137*, 11076−11084.

306   [18]   L.-X. Zhou, J.-Q. Xu, Y.-Q. Zheng, H.-L. Zhu, *J. Coord. Chem.* **2017**, *70*, 3379-3393.

307   [19]   P. F. Shi, B. Zhao, G. Xiong, Y.-L. Hou, P. Cheng, *Chem. Commun.* **2012**, 8231.

308   [20]   W. Liu, Z. Li, N. Wang, X. Li, Z. Wei, S. Yue, Y. Liu, *CrystEngComm.* **2011**, *13*,
309   138-144.

310 [21] B. Zhao, H.-L. Gao, X.-Y. Chen, P. Cheng, W. Shi, D.-Z. Liao, S.-P. Yan, Z.-H.
311   Jiang, *Chem. Eur. J.* **2005**, *12*, 149-158.

312 [22] R. Feng, L. Chen, Q.-H. Chen, X.-C. Shan, Y.-L. Gai, F.-L. Jiang, M.-C. Hong, *Cryst.*
313   *Growth Des.* **2011**, *11*, 1705-1712.

314 [23] V. Skripacheva, A. Mustafina, N. Rusakova, V. Yanilkin, N. Nastapova, R. Amirov,
315   V. Burilov, R. Zairov, S. Kost, S. Solovieva, e. al, *Eur. J. Inorg. Chem.* **2008**, *25*,
316   3957-3963.

317 [24] S. Zhao, X. Lue, A. Hou, W.-Y. Wong, W.-K. Wong, X. Yang, R. A. Jones, *Dalton*
318   *Trans.* **2009**, 9595-9602.

319 [25] Z. Wang, Y. H. Xing, C. G. Wang, X. Q. Zeng, M. F. Ge, S. Y. Niu, *Transition Met.*
320   *Chem.* **2009**, *34*, 655-661.

321 [26] Z.-Y. Li, N. Wang, J.-W. Dai, S.-T. Yue, Y.-L. Liu, *CrystEngComm.* **2009**, *11*, 2003-
322   2008.

323 [27] Y.-Z. Ma, L.-M. Zhang, G. Peng, C.-J. Zhao, R.-T. Dong, C.-F. Yang, H. Deng,
324   *CrystEngComm.* **2014**, *16*, 667-683.

325 [28] W.-T. Chen, S.-M. Ying, D.-S. Liu, Q.-Y. Luo, Y.-P. Xu, *Inorg. Chim. Acta* **2009**,
326   *362*, 2379-2385.

327 [29] J.-W. Cheng, S.-T. Zheng, E. Ma, G.-Y. Yang, *Inorg. Chem.* **2007**, *46*, 10534-10538.

328 [30] W. Dietzsch, P. Strauch, E. Hoyer, *Coord. Chem. Rev.* **1992**, *121*, 43-130.

329 [31] J. C. Trombe, A. Gleizes, J. Galy, *C. R. Acad. Sc. Paris* **1982**, *294-II*, 1369-1372.

330 [32] J. C. Trombe, A. Gleizes, J. Galy, *Inorg. Chim. Acta* **1984**, *87*, 129-141.

331 [33] M. Siebold, A. Kelling, U. Schilde, P. Strauch, *Z. Naturforsch.* **2005**, *60b*, 1149-1157.

332 [34] M. Siebold, S. Eidner, A. Kelling, M. U. Kumke, U. Schilde, P. Strauch, *Z. Anorg.*
333   *Allg. Chem.* **2006**, *632*, 1963-1965.

334 [35] M. Siebold, M. Korabik, U. Schilde, J. Mrozinski, P. Strauch, *Chem. Papers* **2008**,
335   *62*, 487-495.

336 [36] M. Siebold, P. Strauch, *Adv. Coord. Bioanorg. Inorg. Chem.* **2005**, 399-410.

337 [37] J. König, A. Kelling, U. Schilde, P. Strauch, *Molbank* **2016**, *2*, M895.

338 [38] R. S. Czernuszewicz, K. Nakarnoto, D. P. Strommen, *J. Am. Chem. Soc.* **1982**, *104*,
339   1515-1521.

340 [39] B. I. Swanson, C. Machell, G. W. Beall, W. O. Milligan, *J. Inorg. Nucl. Chem.* **1978**,
341   *40*, 694-696.

342 [40] S. Bernal, J. A. Diaz, R. Garcia, J. M. Rodriguez-Izquierdo, *J. Mater. Sci.* **1985**, *20*,
343   537-541.

344 [41] S. Bernal, F. J. Botana, R. Garcia, J. M. Rodriguez-Izquierdo, *J. Mater. Sci.* **1988**, *23*,
345   1474-1480.

346 [42] J. König, *Dissertation: Synthese und Charakterisierung von 3d-4f-Komplexen und*
347   *deren Vorläufer mit 1,2-Dithiooxalat als Ligand*, Potsdam, **2016**.

348 [43] S. Cotton, *Lanthanide and Actinide Chemistry*, John Wiley & Sons, Ltd, Uppingham
349   School, Uppingham, Rutland, UK, **2007**.

350 [44] Q.-Y. Chen, Q.-H. Luo, L.-M. Zheng, Z.-L. Wang, J.-T. Chen, *Inorg. Chem.* **2002**,
351   *41*, 605-609.

352 [45] D. Coucouvanis, N. C. Baenziger, S. M. Johnson, *J. Am. Chem. Soc.* **1973**, *95*, 3875-
353   3886.

354 [46] P. Román, A. Luque, J. M. Gutiérrez-Zorrilla, J. I. Beitia, M. Martínez-Ripoll, *Z.*
355   *Kristallogr.* **1992**, *198*, 213-225.

356 [47] R. D. Shannon, *Acta Cryst.* **1976**, *A 32*, 751-767.

357 [48] R. D. Shannon, C. T. Prewitt, *Acta Cryst.* **1969**, *B 25*, 925-946.

358 [49] R. Mattes, W. Meschede, W. Stork, *Chem. Ber.* **1975**, *108*, 1-5.

359 [50] X-Area, 1.26 ed., Stoe & Cie GmbH, Darmstadt, Germany, **2004**.

360 [51] SHELXS-97, G. M. Sheldrick, University Göttingen: Göttingen, Germany, **1997**.

361 [52] SHELXL-2014/7, G. M. Sheldrick, University Göttingen: Göttingen, Germany,
362   **2014**.

363 [53] DIAMOND, Vers. 4.5.1., K. Brandenburg, Crystal Impact, Bonn, Germany, **2017**.

364 [54] O. V. Dolomanov, L. J. Bourhis, R. J. Gildea, J. A. K. Howard, H. Puschmann,
365   OLEX2, *J. Appl. Cryst.* **2009**, *42*, 339-341.

366   [55]   PLATON, A. L. Spek, Multipurpose Crystallographic Tool, Utrecht University,
367   Utrecht, The Netherlands, **2008**.

368   [56]   C. Matz, R. Mattes, *Z. Naturforsch.* **1978**, *88b*, 461-462.

369   [57]   B. Wenzel, B. Wehse, U. Schilde, P. Strauch, *Z. Anorg. Allg. Chem.* **2004**, *630*, 1469-
370   1476.

371

372